Towards an AMTEC-like device based on non-alkali metal for efficient, safe and reliable direct conversion of thermal to electric power

Gianluca Tumminelli, *Università degli Studi di Palermo (UNIPA), Dipartimento di Fisica e Chimica,* Palermo, Italy, gianluca.tumminelli@unipa.it
Salvatore Ferruggia Bonura, Università degli Studi di Palermo (UNIPA), Dipartimento di Fisica e Chimica, Palermo, Italy, salvatore.ferruggiabonura@unipa.it
Luisa Sciortino, Università degli Studi di Palermo (UNIPA), Dipartimento di Fisica e Chimica, Palermo, Italy, luisa.sciortino@unipa.it
Roberto Candia, Istituto Nazionale di Astrofisica (INAF), Osserv. Astron. di Palermo "G.S. Vaiana", Palermo, Italy, roberto.candia@inaf.it
Ugo Lo Cicero, Istituto Nazionale di Astrofisica (INAF), Osserv. Astron. di Palermo "G.S. Vaiana", Palermo, Italy, ugo.locicero@inaf.it
Fabio Santoro, Archimede S.r.l., Caltanissetta, Italy, santoro@archimede-srl.com
Alfonso Collura, Istituto Nazionale di Astrofisica (INAF), Osserv. Astron. di Palermo "G.S. Vaiana", Palermo, Italy, alfonso.collura@inaf.it
Marco Barbera, Università degli Studi di Palermo (UNIPA), Dipartimento di Fisica e Chimica, Palermo, Italy, marco.barbera@unipa.it

***Abstract*— Alkali Metal ThermoElectric Converters directly convert heat into electric energy and have promising applicability in the field of sustainable and renewable energy. The high theoretical efficiency, close to Carnot's cycle, the lack of moving parts, and the interesting operating temperature range drive the search for new materials able to ensure safe and reliable operation at competitive costs.**

The present work focuses on the design of a non-alkali metal based cell and on the fabrication of a testing device to validate the design work. The selection of a new operating fluid for the cell improves durability, reliability and safety of the device.

Finally, we discuss possible applications to already existing thermal energy sources.

Keywords*— *AMTEC; direct heat-to-electricity conversion; renewable and sustainable energy; model simulations; electrochemical cells; solar energy; biomass; heat waste

I. INTRODUCTION

AMTECs (Alkali Metal ThermoElectric Converters) belong to the category of devices capable to directly convert heat to electricity. To date, this technology has been applied to few space and terrestrial applications [1, 2, 3, 4]. Low durability, low power output/weight ratio, hazardousness and cost limit large scale diffusion. In the following we briefly summarize the status of the art of AMTEC cells and outline the related issues.

Fig. 1 depicts the main components of a common AMTEC multitube cell with natural recirculation system, adopted for space applications [5]. The internal circuit is mainly constituted by both solid electrolytes and their terminals and connectors, which are properly series connected, as well as by porous electrodes in contact with solid electrolytes; the external circuit consists of a variable electric load.

The beta"-alumina solid electrolyte is the heart of the AMTEC cell. In most popular models, it is a solid ceramic β"-alumina [5] tube, a material capable to allow the passage of ions and prevent electron flow, resulting in an electrical insulation behaviour. The outer stainless steel casing includes a bottom cover, which encloses the hottest region, and a top cover, enclosing the coldest region. In the evaporation zone the molten alkali metal vaporises. On the opposite side of the cell, the condenser cools down gas vapours and promotes condensation. The condensed phase is then conveyed into a central channel, leading the fluid back to the evaporator, either by natural or forced circulation. In the configuration of fig. 1 tubular porous electrodes are installed onto the outer and the inner faces of the tubular beta-alumina solid electrolyte (BASE). They are crucial items in the design of an AMTEC and are usually made of molybdenum (Mo), titanium nitride (TiN) or rhodium-tungsten alloys (DSA, Dimensionally Stable Anodes). The cathode is grown on the outer surface of the BASE by chemical deposition of vapours or sputtering, whereas the anode is applied onto the inner surface via Weber process [6] and then coated by molybdenum, in order to prevent electrical leakages. Moreover, a number of thermal shields (not reported in fig. 1) may be installed to limit the parasitic heat loss by radiation.

The alkali metal atoms ionise at the interface between the electrode and the solid electrolyte (oxidation) and pass as positive charge through the solid electrolyte, leaving one or more free electrons onto the porous electrode. Electrons migrate to the porous cathode through the internal and the external electric circuit and they recombine with the cations, producing the neutral alkali metal atom (reduction).

As long as the external electric circuit is open, the charge separation process terminates as soon as the number of excess electrons accumulated at the higher temperature side (anode) and the number of excess cations accumulated at the lower temperature side (cathode) determine an electrochemical equilibrium, preventing further flow of metal ions. When an

external electric load is applied, an electric current is generated and it is possible to exploit the generated electric potential: electrons start to flow through the load, produce electric work and return to the cathode where they recombine with the alkali metal cations.

After recombination, the neutral gaseous alkali metal atoms move towards the condenser, condensate and move by gravity or via a pumping system to the higher temperature region. In this way, a continuous recirculation is guaranteed.

Two main types of AMTEC cycles exist, the so-called liquid-anode and the vapour-anode cycle, depending on the phase of the alkali metal in contact with the anode. The metal used as working fluid also determines AMTEC operating temperatures, which typically range between 900 K and 1,300 K at the hot source (anode), and between 400 K and 700 K at the cold source (cathode).

The expected performance of a saturated vapour-anode/saturated vapour-cathode single-cell AMTEC device operating with alkali metals, as computed by the mathematical model developed in a previous work [7], can be summarised as follows: open circuit voltage ranging from 0.66 V up to 1.20 V, short-circuit current density from 0.11 A/cm^2 up to 1.53 A/cm^2 and maximum power density from to 14.1 mW/cm^2 up to 240 mW/cm^2 depending on the alkali metal used (lithium, potassium, sodium) [7]. Simulation results have been obtained with operation at anodic temperature of 1000 K and cathodic temperature of 500 K, being the operating pressure uniquely determined by the nature of the working fluid adopted, as it coincides with the vapour pressure of the metal itself.

Model simulations confirmed that the electrical performance of a cell, even operating with new working fluids, is a trade-off between the voltage generated by the vapour pressure difference occurring when operating within a temperature range compatible with solar energy concentration systems, on one side, and the solid electrolyte electrical and geometrical features, on the other side, which shall be able to grant good electrical and mechanical performances. Lower ionic conductivity and thicker solid electrolytes lead to greater internal areal resistance which in turn produces higher voltage drops inside the cell itself, at expenses of the useful power density available on external load.

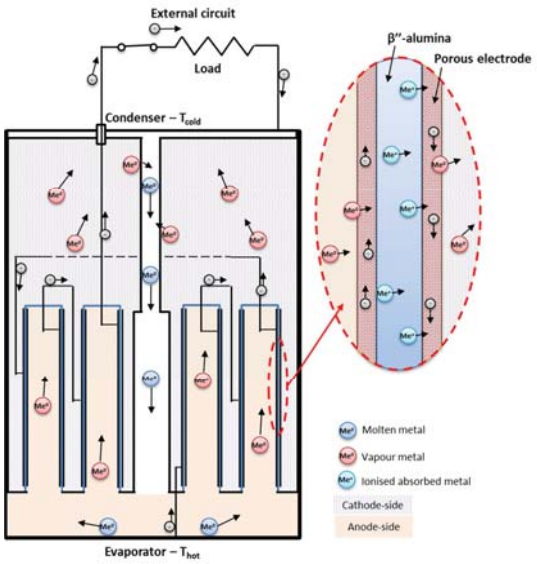

Fig. 1. Simplified drawing of a multitube vapour anode/vapour cathode AMTEC device with indication of main items and operation principle, used for space applications.

In particular, although lithium presents the highest open circuit cell voltage with respect to potassium or sodium, the maximum extractable electric power density is much lower than K- or Na-based cells, at equal working temperatures, due to the higher ionic resistance of Li-based solid electrolytes with respect to other ones. As authors stated in [7], such behaviour is due to kinetic causes, e.g. to the membrane energy barrier E_m and to the sticking coefficient α, introduced in the model in order to describe the energetic and statistic aspects of the phenomena involved in the process. The membrane energy barrier actually depends also on the external load, besides on the BASE ionic conductivity and thickness. Such energetic and statistical approach is valid for both the saturated liquid-anode/saturated vapour-cathode systems (as those described in [8]) and the saturated vapour-anode/saturated vapour-cathode ones modelled in [7]. This suggests that optimal high-performing working fluid-BASE pairs may exist and be particularly suitable for the use in solar-driven Metal ThermoElectric Converters. Moreover, in order to achieve higher, significant and usable power density at practical common operation voltages, a number of cells has to be series connected.

Considering the aggressiveness of metal vapours on both steel and alumina parts and the need to operate at milder temperatures (both aspects affecting the durability of the device), low melting point metals belonging to II B group (Zn, Cd, Hg), III A group (Ga, In, Tl) and IV A group (Sn, Pb) have been identified as potential promising working fluids, deserving more investigations.

In Section II materials and methods deployed in this research work are discussed; the cell model-based simulations are presented in Section III, and cell design and fabrication are described in Section IV; in Section V possible applications to already existing thermal energy sources are discussed while Section VI contains a brief work summary and conclusions.

II. Materials and Methods

A. Working fluids and electrolytes

In order to investigate new potential working fluids, different than alkali metals, new solid electrolytes are needed, properly conditioned or "doped" in compliance with the same diffusing metal ion as the working fluid. Commercially available solid electrolytes can be found, based on sodium, lithium, potassium, barium, strontium, silver and lead (from Ionotec LTD). Unfortunately, no zinc, cadmium, mercury, gallium, indium, thallium, tin based solid electrolytes exist, neither on commercial or laboratory scale, due to lack of market demand, despite some studies on divalent beta"-aluminas can be found in literature [9]. Therefore, the adoption of a system or technology capable to dope already commercially available solid electrolytes is needed.

B. Preparation of doped beta"-aluminas

Beta"-aluminas are excellent conductors for bivalent ions, as demonstrated in [10]. They are prepared starting from a sodium beta"-alumina, by substitution of the sodium cation with cations Ba^{2+}, Sr^{2+}, Cd^{2+}, Hg^{2+}, Pb^{2+}, Mn^{2+}, while the Zn^{2+} beta"-alumina is prepared starting from a Ag^{+} beta"-alumina by substitution of the silver cation with the Zn^{2+} cation.

Table 1. Selected electrical and transport properties of zinc, cadmium and lead based beta"-aluminas.

	Zn β"-alumina	Cd β"-alumina	Pb β"-alumina
Ion conductivity σ [$\Omega^{-1}m^{-1}$] @ 600°C	0.1221	2.171	51.87
Resistivity ρ [Ω m] @ 600°C	8.1917	4.606e-1	1.928e-2
Areal resistance ρ_{areal} [Ω m^2] @ 600°C 0.5 mm thickness	4.096e-3	2.303e-4	9.638e-6
Diffusion coefficient D [m^2/s]	4.648e-12	1.054e-10	-

The greater propensity of silver ions in Ag^+ beta"-alumina to be substituted by Zn^{2+}, with respect to the sodium or lithium ions in Na^+ and Li^+ beta"-aluminas respectively, does not lie with thermodynamics but primarily with kinetic reasons, i.e. with the fact that silver favours the melt phase while sodium and lithium favours the solid phase. At ambient temperature, the ion conductivity of other-than-sodium beta"-aluminas are two orders of magnitude lower than sodium beta"-alumina, while the differences are less evident at temperatures higher than 750 K. As an example, the Pb^{2+} beta"-alumina shows an ion conductivity close to that one of sodium even at temperatures lower than ambient one [9].

Solid electrolytes doped with divalent cations can be obtained either from beta-alumina or from beta"-alumina. Divalent cation-doped beta"-aluminas are kinetically more stable than beta-aluminas and do not show hysteresis phenomena both in heating and cooling. Moreover, unlike doped beta-alumina that may present a certain number of cracked crystals due to ion substitution, as reported by Yao at al. [11], beta"-alumina are not subject to cracking, provided that the difference in ionic radius of the divalent and the monovalent cation is not too large.

The replacement mechanism of the monovalent cation with a divalent one can be either by the simple high-temperature diffusion of divalent metal vapours or by the lower temperature diffusion of cations of a chloride salt of the divalent metal [9]. In some cases, the high vapour pressure of metal salts (e.g. mercury salts) requires the use of ceramic- or quartz-sealed

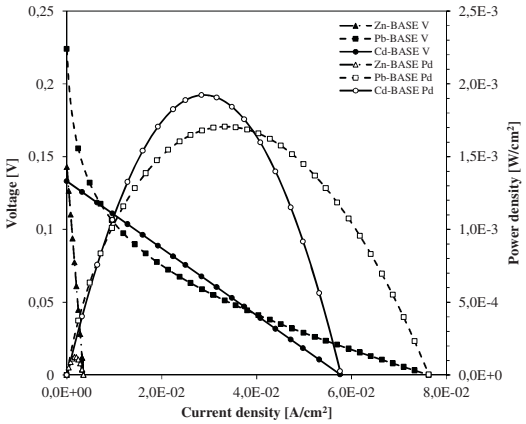

Fig. 2. Computed polarisation and power curves for three different vapour-anode/vapour-cathode AMTEC-type devices, operating with zinc, cadmium or lead vapour, respectively. Simulation parameters: membrane thickness 0.5 mm, anode temperature 973 K, cathode temperature 773 K, $\alpha_a=\alpha_c=1$ (effective adsorption); vapour pressures are computed as function of temperature according to [17].

crucibles and lower temperature process, with consequent lengthening of the diffusion process and, in most cases, a small replacement percentage of the sodium cations.

Dunn et al. [12] demonstrated that beta"-aluminas show very fast diffusion while divalent cations (Ba^{2+}, Sr^{2+}, Cd^{2+}) diffuse more slowly in beta-alumina. Most of divalent cations replace a large percentage of sodium cations in the membrane within the first hour of diffusion and, in some cases, complete substitution can be obtained in few minutes if membranes thinner than 0.2~0.3 mm are used.

C. Estimation of ion conductivity from diffusion data

De Nuzzio et al. [13] and Dunn et al. [14] obtained replacement percentage vs time curves of cadmium, zinc and strontium cations during substitution in sodium beta"-aluminas via radiochemical techniques based on ^{22}Na. The substitution percentage ε% can be described by an expression like:

$$\varepsilon\% = 100 \cdot \frac{2}{L} \int_0^{\frac{L}{2}} \exp\left(-\frac{x^2}{4Dt}\right) dx \qquad (1)$$

in which L is the solid electrolyte thickness, D is the diffusion coefficient and t is time. Expression (1) can be derived analytically from mass balances based on the first and the second Fick's laws, according to the penetration theory [15].

The diffusion coefficient of doping cations in the beta"-alumina was retrieved by best-fitting of experimental data collected at constant temperature. Hence exchange percentage fitted data allow to determine indirectly the diffusion coefficient D of a certain ionic species in beta"-alumina, and this in turn can be related to the ion conductivity σ through the Nernst-Einstein [16] relationship which applies at constant temperature T:

$$\sigma T = nz^2 e^2 \frac{D}{k_B} \qquad (2)$$

where n is the number density (which is a measure of the density of the crystalline lattice), z is the metal ion valency, e is the elementary charge and k_B is the Boltzmann's constant.

The same procedure as reported in [9] has been adopted in the present work, together with experimental data of exchange percentage vs time available from [14], in order to estimate the ion conductivity of zinc, cadmium and lead based beta"-alumina solid electrolytes, which is in turn needed for model simulation of electrical performance of such devices.

Best-fitted values for the diffusion coefficient are $4.648 \cdot 10^{-12}$ m^2/s at T=500 °C for zinc and $1.054 \cdot 10^{-10}$ m^2/s at T=600 °C for cadmium, which lead to ion conductivity of 0.1081 and 2.171 $(\Omega\ m)^{-1}$ respectively. The ion conductivity of lead-doped beta"-aluminas has been derived directly from conductivity vs temperature data from [9], and has been found to be equal to 51.87 $(\Omega\ m)^{-1}$ at T=600 °C. In order to make a comparison between the three different metals at the same temperature, Zn^{2+} β"-alumina conductivity was extrapolated according to equation $\sigma/\sigma_0=T/T_0$, derived from experimental conductivity data reported in [9], resulting in 0.1221 $(\Omega\ m)^{-1}$ at 600°C. Table 1 summarises the adopted electrical and transport properties of Zn, Cd and Pb β"-aluminas.

III. Cell Model Simulations

Model simulations of the Zn, Cd and Pb saturated vapour-anode/saturated vapour-cathode systems, based on the mathematical model developed in [7], have been carried out and produced polarisation and power curves reported in fig. 2.

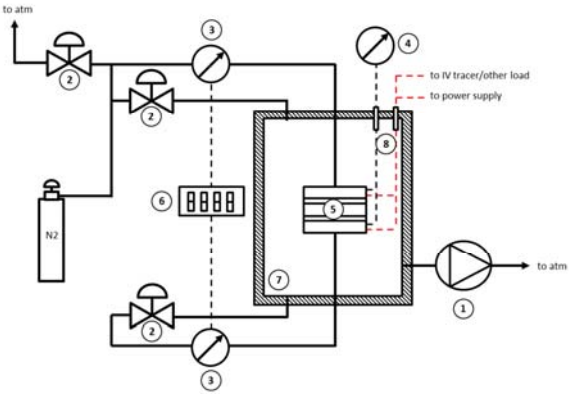

Fig. 3. Simplified sketch of the developed experimental apparatus: (1) vacuum pump, (2) Nupro vacuum valve, (3) pressure gauges, (4) temperature gauges, (5) experimental cell, (6) pressure reader, (7) vacuum chamber, (8) feed-through connections for power supply of electric band heaters and control and measurement signals. In particular, the external electric circuit can be closed either on an I-V tracer device (during measurement test) or on another load (during normal operation).

Anode and cathode temperatures in all cases are set to 973 K and 773 K respectively, while BASE thickness is 0.5 mm and metal vapour pressures are calculated with data reported in [17]. For these simulation, the sticking coefficients are set equal to 1 on both sides of the BASE (effective adsorption), following [8].

As it can be seen, the performances obtainable with divalent cations are qualitatively similar (as expected) to those obtained with monovalent alkali metals (sodium, potassium and lithium) and reported in a previous paper [7].

However, power density values (0.125, 1.92 and 1.71 mW/cm^2 for Zn, Cd and Pb respectively) are definitely much lower than those computed in [7] for a sodium cell (240 mW/cm^2) and even one order of magnitude lower than those computed for a lithium cell (14.1 mW/cm^2), although the durability performance could be better than sodium, considering the chemical aggressiveness of such alkali metal on membrane, electrodes and stainless steel enclosure. This behaviour can be related to the much lower ion conductivity of BASE divalent cations with respect to monovalent cations, being equal the operating temperature. In addition to this, it has to be considered that supply cost of zinc, cadmium and lead is lower than sodium.

Fig. 4. Proprietary developed experimental apparatus with indication of main items: (A) vacuum chamber; (B) experimental cell; (C) vacuum circuit; (D) feed-through system for power, control and signal connections; (E) vacuum pump.

By observing the characteristic parabolas (Fig. 2) describing the power density vs the current density, there is an evident difference in magnitude, with cadmium and lead based systems showing significantly larger values than zinc-based cell. Three different trends have been obtained instead in the polarisation curves of Zn, Cd and Pb systems. Regarding zinc and cadmium systems, the polarisation curve is actually a straight line, the former showing a much higher resistivity with respect to the latter, resulting in a greater slope of the line, - which makes zinc system less suitable for practical applications with respect to cadmium and lead. Lead-based systems provide lower resistivity, especially at normal current density regimes, as demonstrated by the change in slope of the polarisation curve. This suggests, together with the higher useful maximum power density obtainable with respect to zinc, that saturated lead vapour-anode/saturated lead vapour-cathode devices deserve more investigation and could have interesting development.

Results from the planned experimental campaign are necessary to confirm the theoretical model predictions here presented.

Among other metal elements not included in model simulations, tin might have advantages compared to lead, due to the much lower boiling temperature, i.e. higher volatility and higher vapour pressure. Indium, gallium, thallium and all other low-melting point monovalent metals should exhibit higher ionic conductivity and be more suitable for applications in solar concentration systems.

IV. Experimental Apparatus

A. *Basic operation principle*

An experimental apparatus has been proprietary developed in order to carry out measurements of electrical performances of an AMTEC-like single-cell device operating with non-alkaline metals working fluids coupled with the proper BASE, suitable for solar energy applications. The first experimental campaign will be performed using zinc as a working fluid.

With reference to fig. 3, the experimental apparatus is composed of: the cell composed of two symmetric semi-elements (5), designed and manufactured in-house as described in the following; a turbomolecular vacuum pump (1) connected to the vacuum chamber (7) and to the vacuum circuit; four Nupro vacuum valves (2); two Pirani pressure gauges (3) and controller (6); two feedthrough connections for power supply and electrical I-V signals (8); two cell temperature controllers and two K-type thermocouples (4).

It is worth to precise that the vacuum chamber is necessary in such a home-made lab-scale testing device in order to ensure that no air contaminations and leakages occur through the not-perfect seal between the two semi-elements, where the membrane disc is placed. An industrial/commercial version of

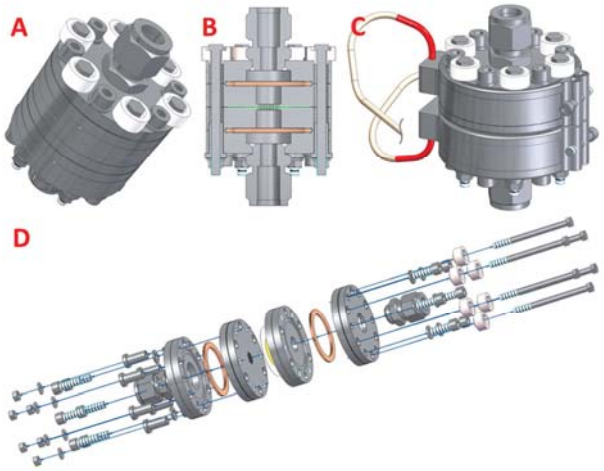

Fig. 5. 3D views of the experimental cell: (A) assembled experimental cell; (B) transverse sectional view with indication of the BASE (green) and ring gaskets (copper); (C) assembled cell with electric band heaters installed; (D) exploded view with focus on bolts assembly.

the device, to be used for power generation only, would not need the extra chamber.

A certain amount of ultrapure solid metal is put inside the two semi-elements of the cell, then the cell is assembled and put inside the vacuum chamber. The chamber is alternatively flushed with gaseous nitrogen and evacuated by the vacuum pump and the operation is repeated 4-5 times in order to remove all traces of air. After the final flush, high vacuum is created inside the chamber by the vacuum pump, and the two semi-cells are heated at two different and constant temperatures by electric band heaters. In this condition, a differential pressure is set across the two semi-elements (i.e. the vapour pressure difference due to the different anodic and cathodic temperatures) which can be fine-tuned and kept constant by regulating the temperature difference.

The external electric circuit is closed either on an I-V tracer during measurement tests, which automatically applies a variable load, ranging from open circuit to short-cut, in order to obtain the polarisation and power curves, or on another electric load, during normal operation.

B. Design and manufacturing of the experimental cell

Fig. 4 shows a picture of the experimental apparatus. Fig. 5 depicts different views of the proprietary experimental cell developed in this work, which has been designed in Siemens SolidEdge ST10 software [18]. In the following, the executive details of the manufacturing of the device are presented.

The electrochemical device is made up of two semi-cells which are electrically separated by a ceramic disc. The semi-cells are constituted by four Conflat DN40 AISI 316L stainless steel commercial flanges.

In particular, as we aim to design a system capable to maintain a differential pressure between the two chambers through a β”-alumina disc, a double drilling on each flange has been done, at the same distance from the existing holes: the first set of holes has a diameter of 8.5 mm while the second one has a diameter of 6.6 mm, separated by a 30° pitch along the circumference. The smaller diameter hole set guarantees the closure of the two flanges which constitute each chamber (semi-cell) while the larger diameter hole set is for clamping the two chambers and maintain the β-alumina disc in position.

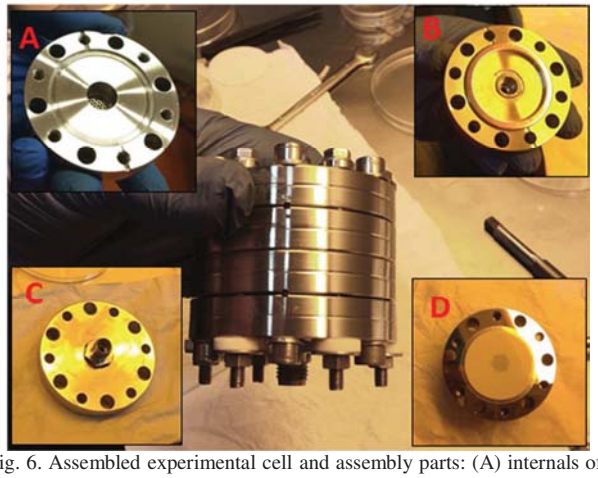

Fig. 6. Assembled experimental cell and assembly parts: (A) internals of the inner flange with view of perforated grid and solid zinc slot; (B) installation of the copper ring gasket on the internal face of outer flange; (C) external face of outer flange, (D) placement of the membrane on the external face of inner flange.

The Conflat flanges include a circular slot where proper DN40CF copper ring gaskets are placed, in order to ensure a hermetic sealing towards the external environment.

An additional hole for the installation of an O.D. 1/4” stainless steel tube is realised on the outer flange, for the connection to the external vacuum circuit.

To let the alkali metal be positioned inside the semi-cell, on the two inner flanges of chambers, a circular 10 mm deep compartment has been realised. The chamber wall facing the β”-alumina disc on both chambers has been perforated with an hexagonal pattern grid of circular holes, having a diameter of 1.2 mm each and a pitch of 1.5 mm.

When assembling the two semi-cells 6 cylindrical Macor insulators (o.d. 8 mm, i.d. 4.5 mm) have been used together with 6 hexagonal screws and 6 nuts, in order to ensure electrical insulation and good clamping between the semi-elements. The assembly parts of the semi-cell are reported in fig. 6 together with the assembled experimental cell.

Two 400W band electric heaters are clamped to the two semi-elements in good thermal contact with the lateral surface of the semi-cells. Such heaters provide the thermal energy needed to maintain a constant temperature inside the cell, which in turn determines the vapour pressure of the metal investigated as working fluid. The heating system is completed by two K-type thermocouples directly screwed onto the anodic and cathodic outer flanges, and connected to a temperature controller which switches the heaters on and off to maintain a constant temperature set point.

The mass transfer from the hot, high pressure semi-element to the cold, low pressure one leads to the progressive depletion of the metal mass in the hot semi-element, which passes into the cold one through the membrane until the pressure in the hot semi-element falls below the vapour pressure that the element would have at the anodic temperature. The device does not include a re-circulation system from the cathodic chamber back to the anodic chamber and thus it cannot work as a renewable battery producing electric power over a long time, however, it works as a test device for a sufficient time to perform the material characterizations. Basically, the electrical characteristic of the cell remains constant as long as the amount of metal is sufficient to ensure a two-phase system (liquid-vapour equilibrium) in both semi-elements.

V. Potential application to solar energy

The simple design proposed in the present work would simplify the manufacturing of the cell, reduce costs and make it suitable to combined application with discontinuous heat source, as solar radiation.

In fact, both in parabolic linear and parabolic dish solar collectors, the optical focus has got different positions during the day, as it tracks the relative sun position. Due to the effect of gravity, if one or more cells are installed on the focus, then they could have part of the BASE wetted by the melted metal, both at anode and cathode side, being the remaining part in contact with the vapour metal. In a well-designed cell, instead, the BASE would be in contact with metal vapours only for most of the operation during the day.

In a Fresnel-type solar collector, on the other hand, the optical focus does not change its absolute position during the day, as the maximisation of the solar energy capitation lies with the movable mirrors system.

For these reasons the saturated vapour-anode/saturated vapour-cathode configuration seems more indicated for coupling with parabolic linear or parabolic dish collectors, while the saturated liquid-anode/saturated vapour-cathode configurations are particularly suitable for coupling with Fresnel-type solar collection systems. Moreover, both types of AMTEC-type cells can also be easily coupled to waste heat recovery systems as well as to biomass and biogas heat production.

In any case, when applying such a device to any thermal energy available source, a regeneration or recirculation system, like those already provided in current AMTECs, has to be adopted in order to get a continuous operation. Our investigated regeneration/recirculation system will be discussed in another paper.

VI. Summary and Conclusion

The present work focused on the design of a non-Alkali Metal ThermoElectric cell, based on the same AMTEC operation principle but operating with some other cheaper and more durable and reliable non-alkali monovalent or divalent low melting point metals belonging to II B group (Zn, Cd, Hg), III A group (Ga, In, Tl) and IV A group (Sn, Pb).

The fabrication of a home-made, lab-scale testing device followed in order to validate the design work and start experimental measurements of cell electric performance, whose results will be necessary to confirm the theoretical model predictions.

Vacuum tests assessed the absence of air leakages and contaminations from the external ambient into the device.

Finally, we briefly discussed about the possible application of such developed device to already existing eco-friendly thermal energy sources, such as solar radiation collection systems, biomass and biogas power systems.

Acknowledgments

The present research described in the present work has been developed during the PhD course in Physics, XXX cycle, International Curriculum in Statistical and Interdisciplinary Physics, at Università degli Studi di Palermo. The research activity has been supported by Istituto Nazionale di Astrofisica (INAF), XACT Laboratory (Palermo, Italy), and has been partially funded by Qohelet Solar Italia S.p.A. (Caltanissetta, Italy). Special thanks to Ionotec Ltd. (Runcorn, Cheshire, England) for the BASE supply and Archimede S.r.l. (Caltanissetta, Italy) for the technical and scientific support.

References

[1] M. Underwood, B. Jeffries-Nakamura, D. O'Connor, M. Ryan, J. Suitor and R. Williams, "A five-volt AMTEC multicell," *American Chemical Society: Washington DC,* vol. 1, pp. 855-859, 1993.

[2] M. Yoichi and M. El-Genk, "Electrical breakdown experiments with application to alkali metal thermal-to-electric converters," *Energy Conversion and Management,* vol. 44, pp. 819-843, 2003.

[3] M. El-Genk, J. Tournier, J. King and Y. Momozaki, "Novel, Integrated Reactor/Power Conversion System (NIR/PCS): Alkali Metal Thermal-To-Electric Energy Conversion Progress Report Performance Period: September 1999–August 2000. Report No. UNM-ISNPS-3-2000," *The University of New Mexico's Institute for Space and Nuclear Studies, Albuquerque, NM,* 2000.

[4] M. El-Genk, J. Tournier and Y. Momozaki, "Novel, Integrated Reactor/Power Conversion System (NIR/PCS): Design and Analyses of Alkali Metal Thermal-To-Electric Conversion Units and Interfacing with Nuclear Reactor, Progress Report II. Report No. UNM-ISNPS-2-2001," *The University of New Mexico's Institute for Space and Nuclear Studies, Albuquerque, NM,* 2001.

[5] S.-Y. Wu, L. Xiao and Y.-D. Cao, "A review on advances in alkali metal thermal to electric converters (AMTECs)," *Intern. Journ. of Energy Research,* 2009.

[6] M. Lodhi and J. Briggs, "The Grain Size Effect on Thermo-chemical Properties of AMTEC electrodes," *Int. J. Electrochem. Sci.,* vol. 2, pp. 469-477, 2007.

[7] G. Tumminelli, R. Candia, A. Collura, U. Lo Cicero, L. Sciortino, S. Ferruggia Bonura, F. Santoro and M. Barbera, "A thermodynamic-statistical model of the electrical characteristics of a 2nd generation AMTEC-type cell for the renewable heat-to-electrical energy direct conversion," *to be submitted,* 2018.

[8] T. Cole, "Thermoelectric Energy Conversion with Solid Electrolytes," *Science,* vol. 221, no. 4614, 1983.

[9] G. Farrington and B. Dunn, "Divalent Beta"-Aluminas: High Conductivity Solid Electrolytes For Divalent Cations," *Soilid State Ionics,* vol. 7, pp. 267-281, 1982.

[10] B. Dunn and G. Farrington, "Fast Divalent Ion Conduction in Ba++, Cd++ and Sr++ Beta"-Aluminas," *Mat. Res. Bull.,* vol. 15, pp. 1773-1777, 1980.

[11] Y.-F. Y. Yao and J. Kummer, "Ion exchange properties of and rates of ionic diffusion in beta-alumina," *Journal of Inorganic and Nuclear Chemistry,* vol. 29, pp. 2453-2466, 1967.

[12] B. Dunn, R. Ostrom, R. Seevers and G. Farrington, "Divalent cation conductivity in beta″ alumina," *Solid State Ionics,* vol. 5, pp. 203-204, 1981.

[13] J. De Nuzzio, R. Seevers, G. Farrington and B. Dunn, "Ion Transport in Ca++, Sr++, Ba++ and Pb++ Beta" Aluminas," *Journal of Solid State Chemistry,* vol. 50, pp. 146-152, 1983.

[14] B. Dunn, B. Karcher and G. Farrington, "Unpublished results".

[15] R. H. Perry and D. Green, "Perry's Chemical Engineering's Handbook 8th ed.".

[16] J. O. Bockris, Modern electrochemistry: funndamentals of electrodics, Springer, 2000.

[17] C. B. Alcock, V. P. Itkin and M. K. Horrigan, "Vapour Pressure Equations for the Metallic Elements: 298-2500 K," *Canadian Metallurgical Quarterly,* p. 309, 1984.

[18] Siemens Solid Egde ST10, "https://www.plm.automation.siemens.com/it/products/solid-edge/," 2018. [Online].

[19] R. K. Sievers, T. J. Hendricks and J. C. Giglio, "Evaporation front position control in alkali metal thermal electric conversion (AMTEC) cells". Patent US5939666 A, 1997.